# NUCLEAR REACTIONS--THEORY

# A MACROSCOPIC APPROACH TO HEAVY-ION COLLISIONS AND FISSION

S.P. Angius and A. Bonasera

It has recently been shown[1-3] that, by making use of the Vlasov equation,[4] it is possible to reduce TDHF to a classical form also in the case of two colliding nuclei. For a situation where a neck is formed between the two nuclei, the following equation can be derived:

$$\frac{d\vec{p}_A}{dt} = \pi r_N^2 \hat{n} \cdot \left[\bar{\bar{\Pi}} + \bar{T}\left(\rho \frac{\partial U}{\partial \rho} - U\right)\right]_{NM} +$$

$$+ 2\pi\sigma r_N \hat{n} + \text{Coulomb force.} \qquad (1)$$

Here, the subscript NM refers to the nuclear matter approximation which is introduced when the TDHF density matrix is substituted by its value in bulk nuclear matter. The second term is the surface contribution, and is proportional to $\sigma$, the surface energy, which is given by

$$\sigma = 0.9517[1 - 1.7826\ I^2]\text{MeV/fm}^2 \qquad (2)$$

This expression is applied to the description of the dynamics of heavy-ion collisions and fission.

In the case of symmetric fission, the results obtained for the kinetic energy released are plotted in Fig. 1 for different values of the neck radius at scission.

The classical equation of motion can also be applied to the case of fusion and fast fission. In this case, we introduce the mass asymmetry degree of freedom, given by the expression:

$$\ddot{A}_1(t) = -\frac{A_1(t)}{\tau} \qquad (3)$$

The distributions thus obtained compare well with the experimental ones.

These calculations show that the classical limit of TDHF gives a good description of nuclear dynamics. For the case of symmetric fission, we have presented a simple, parameter-free model which is in good agreement with TDHF and experimental results.

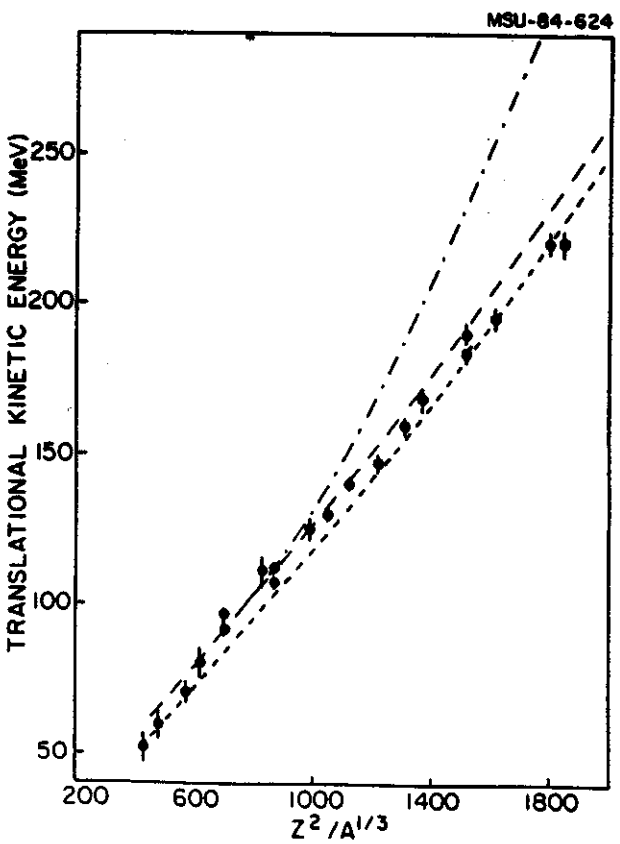


Fig. 1 Translational kinetic energy for symmetric fission versus $Z^2/A^{1/3}$. Short-dashed and long-dashed lines refer to the cases where scission occurs for neck radii less than 0.8 fm and 1.2 fm, respectively. The dotted-dashed line refers to the case of zero friction and scission occurring for a neck radius less than 1.2 fm. Experimental data are from Ref. 5.

1. A. Bonasera et al., Phys. Lett. 141B, 9 (1984).
2. A. Bonasera, Nucl. Phys. A, in press.
3. A. Bonasera, invited talk at the Symposium "Heavy Ion 84", Mt. Fuji, August 1984.
4. A. Bonasera et al., Nuovo Cim. 69A, 69 (1982) and references therein.
5. V.E. Viola, At. Data Nucl. Data Tables 1, 391 (1966).

# HEAVY ION DYNAMICS IN A TDHF-BASED CLASSICAL DESCRIPTION

A. Bonasera

We reduce the TDHF equations of two colliding nuclei to a classical form. These equations mimic the actual behavior of finite nucleus TDHF quite well. The calculated fusion cross sections are in good agreement with experimental data for light and heavy nuclei. The fusion threshold for heavy nuclei is well above the interaction barrier, in agreement with the "extra push" systematics. An interesting feature of our approach is the clear distinction of two different states after neck formation The first stage is superfluid, while in the second stage there is a strong damping (superviscosity). The occurrence of superviscosity in the rebounding phase is not sufficient to give cold fusion in heavy systems, but does result in a long interaction time. This could be a signature of fast fission. At higher energies the approaching phase is entirely superfluid and explains the window in the fusion cross section seen in TDHF for light nuclei.

The process of deep inelastic scattering is well reproduced by the model, but for $E_{lab}$~10 MeV/A the energy loss is largely underestimated. This could be due to the emission of light particles during the first stage of the reaction. The recently observed mass drift away from symmetry supports this conclusion.

---

1. A. Bonasera, Nucl. Phys. A in press.
2. A. Bonasera, Invited talk presented at the Symposium "Heavy Ion 84", Mt. Fuji, August 27-31, 1984; and to be published in the proceedings of the conference.

# BOMBARDING ENERGY DEPENDENCE OF THE EXTENDED PERIPHERAL MODEL

E. Deci and G. Caskey

Friedman's peripheral model[1] of projectile fragmentation has been succussful in describing the energy dependence of quasi-elastic-peak momentum widths, which are observed in heavy ion reactions. This model can be combined with kinematics of the fragmentation process to give peak energies as well as momentum widths for the high energy portion of the observed quasi-elastic peaks. In essence, the succiss of this peripheral model rests in the inclusion of first order nuclear structure effects beyond those of the fermi-gas type calculation employed by Goldhaber[2]. Recently, Deci et al.[3] have studied how proper inclusion of energy conservation and, also, finite geometry effects resulted in remarkable agreement of this model prediction with their $^{14}N + ^{165}Ho$ inclusive fragment data at 20 MeV/nucleon. Caskey et al.[4] recently obtained similar data at 35 MeV/nucleon. We shall compare the prediction of the extended peripheral model with the data at both 20 and 35 MeV/nucleon bombarding energy to observe any differences in agreement between the theory and data. Differences in agreement between the data and theory from one bombarding energy to another may suggest changes in the reactio mechanism as a function of projectile bombarding energy.

Figure 1 shows the 20 MeV/nucleon data of Deci et al.[3] for $^{10}B$ and $^{11}B$ together with the 35 MeV/nucleon data of Caskey et al.[4] for the same isotopes. Note that the predictions (solid lines) agree reasonable for all cases, but there

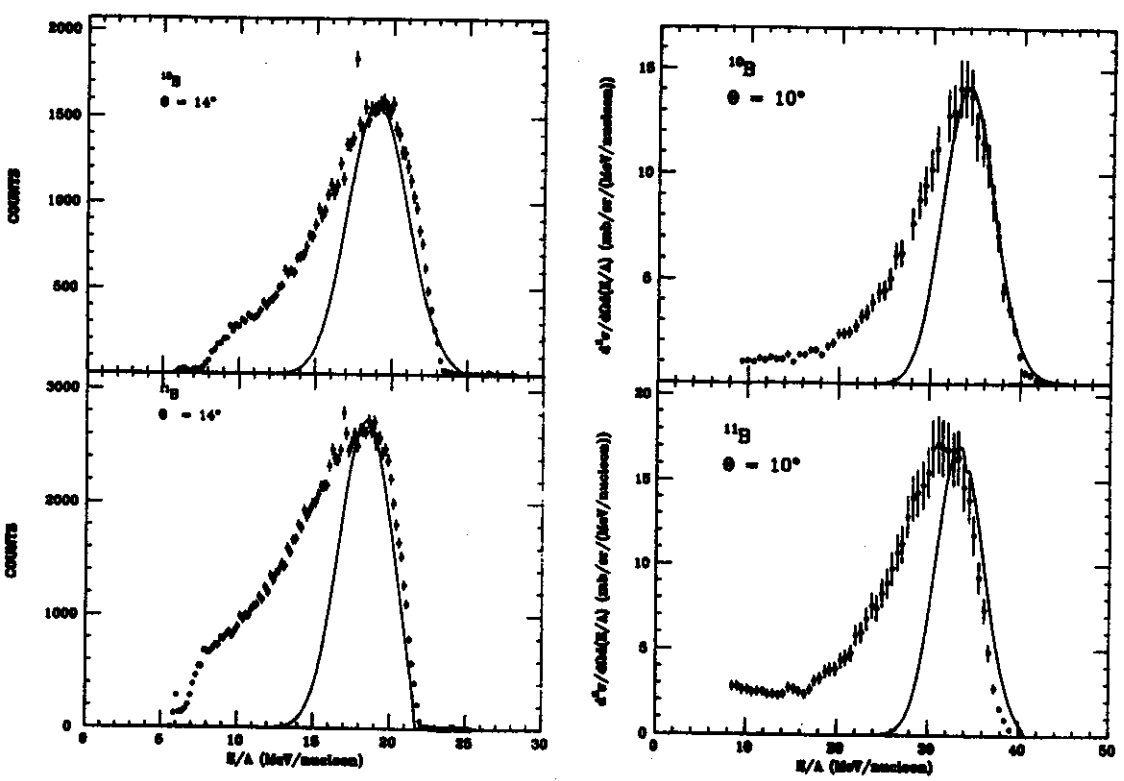


Fig. 1 Fragment energy spectra for two boron isotopes at 20 MeV/nucleon (left) and 35 MeV/nucleon (right). The data at the lower energy were at $\theta_{lab}$=14° and the 35 MeV/nucleon data were obtained at $\theta_{lab}$ = 10° (grazing angles are about 12° and 8°, respectively). The solid lines are predictions of the extended peripheral model.

are some differences between the two energies. At 20 MeV/nucleon the model predicts peaks which are consistently a bit lower in energy than the data, but at 35 MeV/nucleon we see no such trend. In fact, at 35 MeV/nucleon the prediction agrees with the $^{10}B$ data, but the data for $^{11}B$ peaks at a lower energy than the prediction. Errors in the energy calibration for either set of data could be responsible for small systematic shifts of the data relative to the model prediction. However, what we observe is that at 20 MeV/nucleon the predicted peak lags the data by just a bit, and by about the same amount for both $^{10}B$ and $^{11}B$ fragments. But at 35 MeV/nucleon there is a difference in agreement of the model with the data for the two isotopes. This may reflect differences in the underlying reaction mechanism at these two bombarding energies, at least for $^{11}B$ production, though such a conclusion is speculative at this point.

The extended peripheral model is successful in reproducing the quasi -elastic peaks of fragmentation spectra at both 20 MeV/nucleon and 35 MeC/nucleon. The approximations in the model calculation lead to a slight energy dependence of the fit with better agreement occuring at the higher mechanisms in a given channel may be indicated in cases where agreement of the calculation has a strong energy dependence.


1. W.A. Friedman, Phys. Rev. C 27,569(1983).
2. A.S. Golhaber, Phys. Lett. 53B,306(1974).
3. E. Dect, et al., elsewhere in this annual report.
4. G. Caskey, A. Galonsky, B. Remington, M.B.Tsang, C.K. Gelbke, A. Kiss, F. Deak, Z. Seres, J.J. Kolata, J. Hinnefeld, and J. Kasagi, Phys. Rev. C in press.

# CAN WE EXTRACT THE EQUATION OF STATE FROM PION MULTIPLICITIES?

D. Hahn and H. Stöcker

We have carefully studied the recent attempts of Harris et al.[1] and Sano et al.,[2] who claim to deduce the nuclear equation of state (EOS) from pion-multiplicity data[3] within a hydrodynamical model, following the suggestions of Stöcker et al.[4]

To this end we have considered nuclear matter as a relativistic, interacting Bose- and Fermi-gas of π-mesons, η-mesons, photons, and nucleonic resonances up to 2.5 GeV. We regard the first stage of central collisions of two nuclei as the origin of a shock front and solve the hydrodynamical Rankine-Hugoniot equation[5]

$$W^2(\rho,T) - W_0^2 + P\,(W/\rho - W_0/\rho_0) = 0$$

$$W_0 = m_0c^2 - B \qquad (B=16\ \text{MeV})$$

for all interesting bombarding energies. Assuming that the mesons and the nucleonic resonances are in thermal and chemical equilibrium in the shock front and freeze out when the system begins to expand[1,6] we obtain pion multiplicities per nucleon. The exclusive measurements of Ref. 3 have selected central collisions and therefore can be directly compared with the calculations. The nuclear EOS, often referred to as compression energy

$$W(\rho,T=0) - W(\rho_0,T=0) = E_c(\rho)$$

enters the calculation as an interaction energy of the baryonic phase in a self-consistent manner. For details see Refs. 7,8, and 9. We claim that the compression energy was not treated self-consistently in Refs. 1 and 2 and that one has to include the Bose-ground-state for the pions and nucleonic resonances above 1232 MeV. The latter effects increase the pion multiplicity, roughly 15% at $E_{Lab}$= 1 GeV, more at other energies.

We have used two different functional forms as ansatz for $E_c(\rho)$, namely

$$E_c(\rho) = K_1(\rho-\rho_0)^2/18/\rho/\rho_0$$

$$E_c(\rho) = K_q(\rho-\rho_0)^2/18/\rho_0/\rho_0$$

and adjusted the compression constants K to the data. Our results (see Fig. 1) show that we can fit the pion multiplicities between 300 and 2000 MeV with both the functional forms for $E_c$ with $K_1$=1400 MeV and $K_q$ =800 MeV. Nonetheless, the two equations of state, which we obtain by this procedure, are substantially different (Fig. 2)

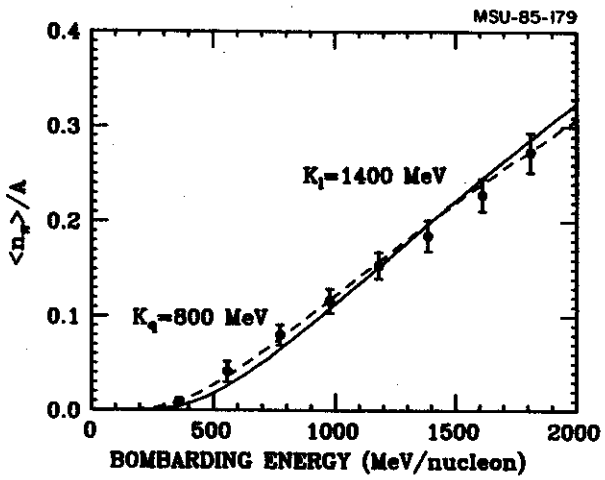


Fig. 2. The equations of state for $K_l$=1400 MeV and $K_q$=800 MeV at the energies of the exclusive pion multiplicities of Ref. 2. Circles refer to the linear, triangles to the quadratic EOS.

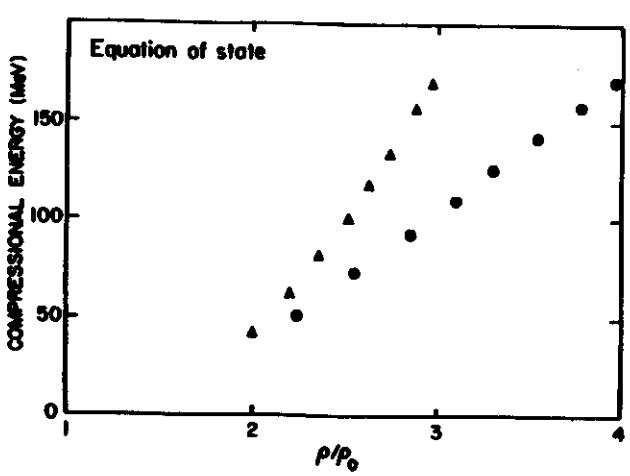


Fig. 1. Pion multiplicities per nucleon for central collisions in the $^{40}$Ar+KCl system. The data of Ref. 2 are compared with the results of the shock calculations. The full curve shows the results for the linear EOS with $K_l$=1400 MeV, the dashed curve the results for the quadratic EOS with $K_q$=800 MeV.

and we have to conclude that the EOS cannot be derived unambiguously from the data of Ref. 3. To explain our disagreement with the conclusions of Refs. 1 and 2 and the predictions of Ref. 4, we have shown that the thermodynamical quantity, which determines the pion yields, is the freeze-out temperature of the hadronic system, while the freeze-out density has almost no influence in the energy region of the BEVALAC (Fig. 3). Hence, we can extract from the pion multiplicities at a fixed bombarding energy the temperature, therefore the thermal energy and the nonthermal (compressional + flow) energy, which in our attempt and in those of Harris and Sano is set equal to $E_C$.

We cannot derive, however, the density of the system. This becomes obvious by carefully looking at Fig. 2. The compression energy, calculated with the two different functional forms for $E_C$, is almost the same for the 8 data points, but we have large differences in the densities. Both functional forms are able to give the right dependence $T(E_{Lab})$ in this energy region and reproduce the data, regardless of the density achieved.

After the connection between the pion multiplicities and the thermodynamical properties of hadronic matter has become clear, we have extended our calculations to lower and higher energies. Inclusive measurements of pion cross sections[10,11] have been used with the cross sections for protons of Ref. 11 to get estimates of pion multiplicities at low energies for head-on collisions. The comparison with the pion yields over 8 orders of magnitude shows that the shock calculation works well between 30 MeV and 3000 MeV (see Fig. 4) at least for the quadratic EOS. Within the same energy range, we then have extracted the freeze-out temperature from the pion data, assuming a freeze-out density between 1 and $4\rho_0$ (see Fig. 5). Also it now seems possible to distinguish between different forms of the EOS with data at very low or very high energies. The large discrepancies between the linear and the quadratic form are,

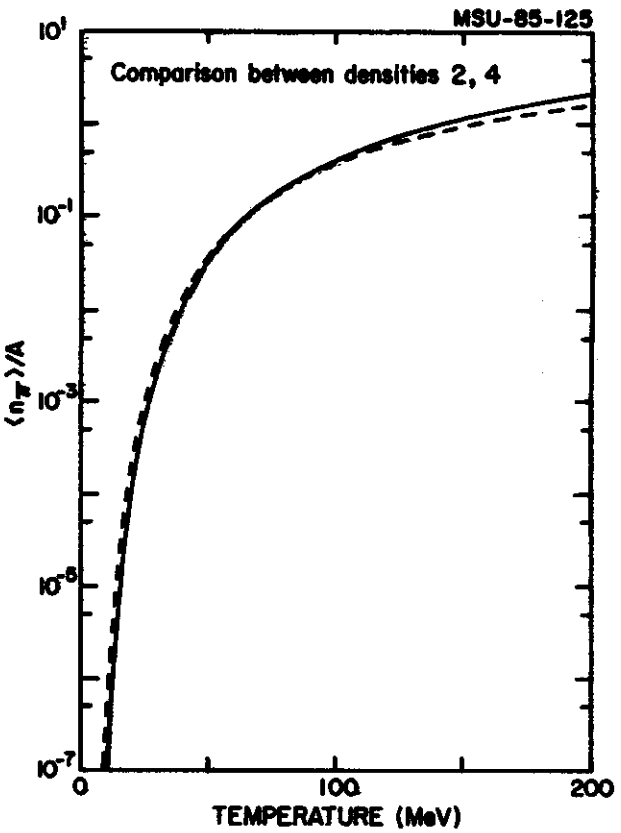


Fig. 3. Pion multiplicities per nucleon versus the temperature of a $^{40}$Ar+KCl system for fixed densities. A fireball model is used without assumptions about the collision process. The full curve represents the density $2\rho_0$, the dashed one $4\rho_0$.

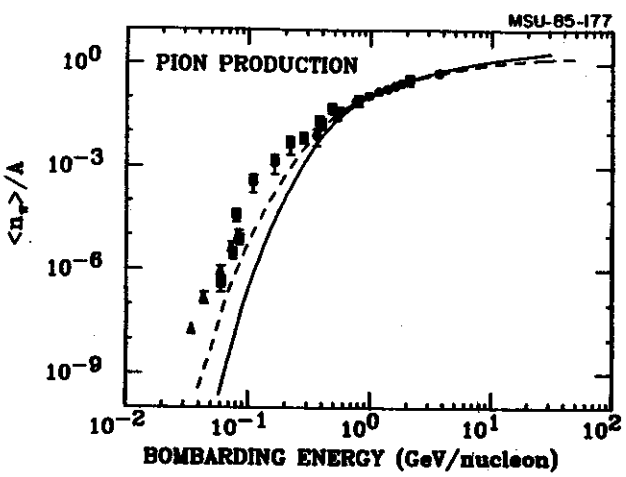


Fig. 4. The same theoretical curves as in Fig. 1, extended over a large energy-scale. The data are taken from Refs. 2, 10, 11 and 12. Circles refer to exclusive $\pi$-measurements, squares to inclusive charged pion yields and triangles to inclusive $\pi^0$-measurements. For details, see Ref. 9.

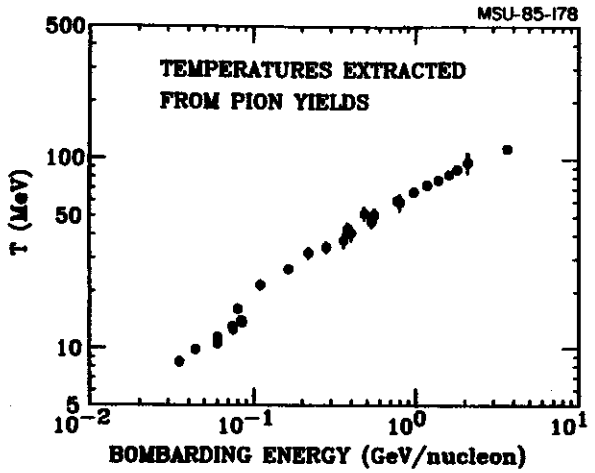


Fig. 5. Temperatures calculated from pion multiplicities. For each bombarding energy, we have assumed the density to be between $\rho_0$ and $4\rho_0$ and have taken into account the experimental errors. No shock calculation but a simple Fireball model was used (see Fig. 3).

however, mostly due to different functions $T(E_{Lab})$ and not to a density-dependence of the pion multiplicities. Other quantities like the flow angle have to be taken into consideration besides the pion multiplicities, to determine the equation of state (see e.g. Ref. 13).


1. J. Harris et al, Phys. Lett., in print
2. M. Sano et al, Phys. Lett., in print
3. A. Sandoval et al, Phys. Rev. Lett. 45, 874 (1980)
4. H. Stöcker et al, Z. f. Phys. A286, 121 (1978)
5. W. Scheid et al, Phys. Rev. Lett. 32, 741 (1974)
6. R. Stock et al, Phys. Rev. Lett. 49, 1236 (1982)
7. U. Heinz et al, J. Phys. G, 5, 1383 (1979)
8. H. Stöcker et al, Z. f. Phys. A303, 259 (1981).
9. D. Hahn and H. Stöcker, to be published
10. W. Benenson et al, Phys. Rev. Lett. 43, 683 (1979), Phys. Rev. Lett. 44, 54 (1980); H. Heckwolf et al, Z. f. Phys. A315, 243 (1984); B. Jakobsson, Phys. Scripta T5, 207 (1983); H. Noll et al, Phys. Rev. Lett., 15, 1284 (1984); J. Stachel, Invited talk at the 7th High Energy Heavy Ion Study, GSI, Darmstadt, Oct. 1984; J.P.Sullivan et al, Phys. Rev. C25, 1499 (1982).
11. S. Nagamiya et al, Phys. Rev. C24, 971 (1981)
12. M. Kh. Anikina et al, Z. f. Phys. C9, 105 (1981).
13. H. Kruse et al, Phys. Rev. Lett. 54, 289 (1985) and in text P. Braun-Munzinger et al, Phys. Rev. Lett. 52, 255 (1984).

# PROBING NUCLEAR MATTER UNDER EXTREME CONDITIONS--TOWARDS THE NUCLEAR EQUATION OF STATE

J.J. Molitoris and H. Stöcker

Very promising progress has been made in studying nuclear matter via two microscopic theories: the Newtonian Classical Equation of Motion approach[1] and the Vlasov-Uehling-Uhlenbeck theory.[2] The collective sidewards flow of nuclear matter, an original prediction of nuclear fluid dynamics,[3] has been observed experimentally[4] and explained theoretically by these two theories.[1,2]

The Newtonian force approach, in which the nucleus is modeled as a system of nucleons, self-bound by a classical two-body potential, provided a dramatic explanation of collective sidewards flow as arising from the repulsive component of the nuclear force for the first time at the microscopic level. See Fig. 1 in which we show a Nb(400 MeV/N)+Nb at b=3 fm. This intrinsically classical approach, which trivially includes Coulomb interactions, is just beginning to shed light on the nuclear matter phase diagram. Predictions concerning the liquid-gas phase transition are forthcoming.

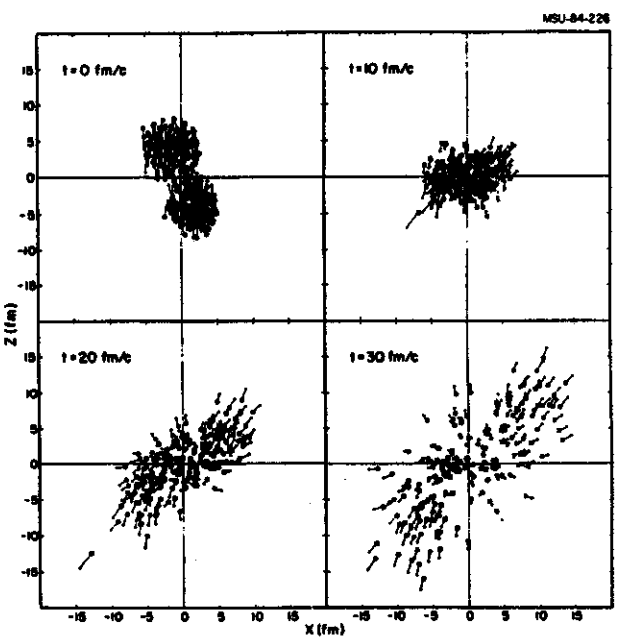


Fig. 1. Nb(400 MeV/N)+Nb molecular dynamics.

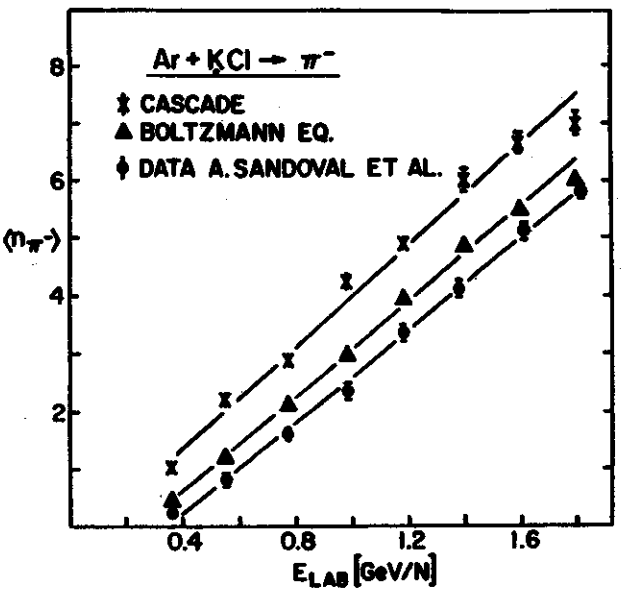


Fig. 2. Vlasov-Uehling-Uhlenbeck pion multiplicities.

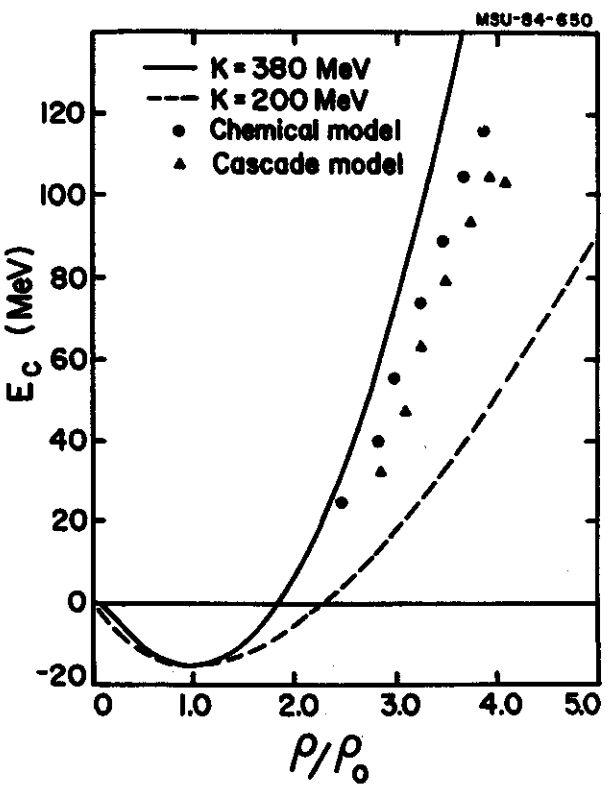


Fig. 3. VUU extraction of nuclear equation of state.

The Vlasov-Uehling-Uhlenbeck theory incorporates mean field dynamics, two-body collisions, and the Pauli principle and so has already provided insight into the importance and interplay of these effects in the 50 MeV/N to 5 GeV/N range. Proton (730 MeV/N) + nucleus collisions have formed a testing ground for the theory and led to an explanation of the target mass dependence and difference in $\pi^+/\pi^-$ yields plus the energy dependence of $\pi^-$ multiplicities from Ar (300 MeV/N to 2 GeV/N) + KCl (Fig. 2). A surprisingly stiff (k=380 MeV) equation of state is an essential ingredient (Fig. 3). The VUU theory mimics TDHF quite well at low energies: without the collision term, the Vlasov equation is recovered (Fig. 4). At higher energies the proper hydrodynamic limit is apparently approached; this microscopic theory also has the compressional energy which causes collective sidewards flow. Symmetric systems such as Ca+Ca, Nb+Nb, Au+Au, and U+U are being studied from 100 MeV/N to 1 GeV/N and preliminary results indicate that the experimental data are explained quite well by this theory (Fig. 5).

The stiff nuclear equation of state is again necessary to explain the collective flow of nuclear matter away from the high density and pressure interaction zone achieved in nucleus-nucleus collisions. Collective flow in light systems at GeV/N energies is detected and

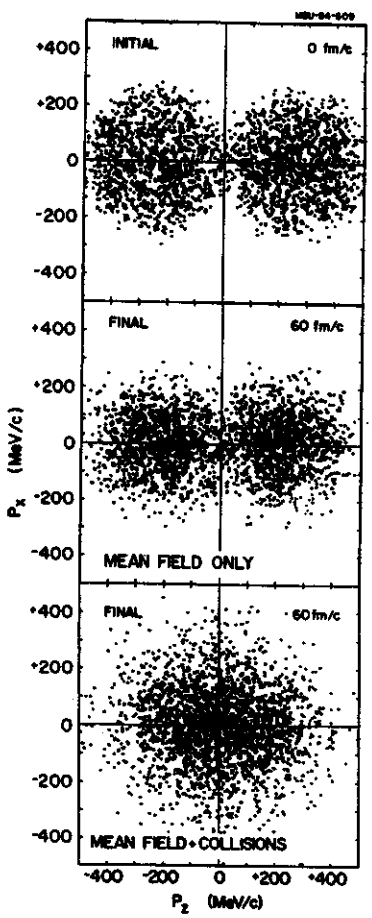


Fig. 4. Strong equilibration predicted by VUU.

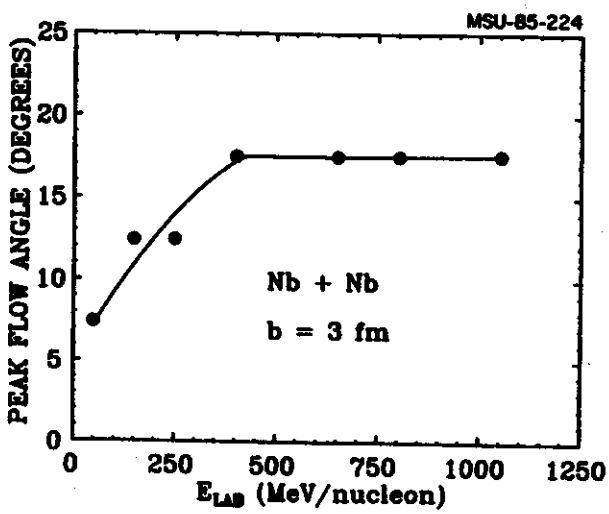


Fig. 5. Energy dependence of flow angle.

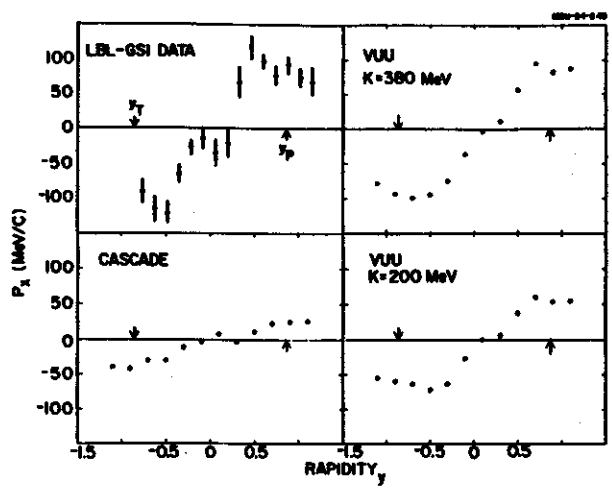


Fig. 6. Sensitivity of transverse momentum spectra to EOS.

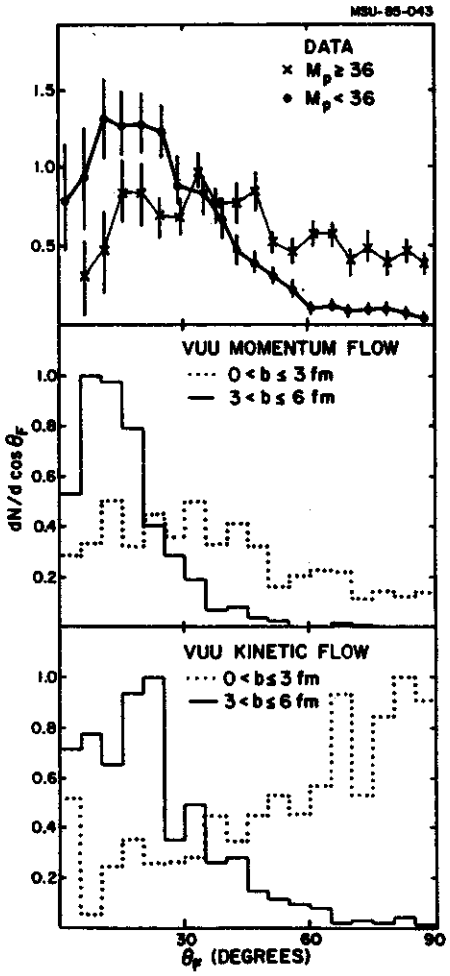


Fig. 7. Ar(770 MeV/N)+Pb flow angle distributions.

explained in the context of the VUU theory with the novel transverse momentum analysis technique of Danielewicz and Odyniec (Fig. 6).[5] Asymmetric systems are studied and understood by applying the usual kinetic energy flow analysis in a new way--only the forward or projectile-like momentum hemisphere is analyzed--the sidewards splash of the projectile is then easily observed (Fig. 7).[6] The VUU theory with appropriate modifications of the initial conditions is also being applied to the problem of phase transitions in nuclear matter.

---


1. J.J. Molitoris, J.B. Hoffer, H. Stöcker, Phys. Rev. Lett. 53, 899 (1984).
2. H. Kruse, B. Jacak, H. Stöcker, Phys. Rev. Lett. 54, 289 (1985).
3. G. Buchwald, et al., Phys. Rev. Lett. 52, 1594 (1984).
4. H. Gustafsson, et al., Phys. Rev. Lett. 52, 1590 (1984).
5. J.J. Molitoris and H. Stöcker, MSUCL-501.
6. J.J. Molitoris and H. Stöcker, MSUCL-503.

# A CONSTRAINED HARTREE-FOCK MODEL FOR THE VAPORIZATION OF HOT NUCLEI

H. Sagawa and G. F. Bertsch*

The theory of nuclear disassembly at high excitation energy is currently a topic of considerable interest. Both statistical and dynamic models have been employed to describe the process. The initial expansion requires a calculation of dynamics such as given by mean field theory[1,2] or classical equations of motion.[3] We know that mean field theory works very well at nuclear matter density, and the finite-temperature generalization should be equally valid for the single-particle density matrix. Of course at low density, Hartree-Fock theory breaks down as clustering becomes important. However, we do expect constrained Hartree-Fock theory to describe the separation of the system into a vapor and a liquid. Our aim is to apply that theory to calculate the fraction of nucleons that are left in the residual nucleus after the expansion phase.

A basic assumption of our model is that the system maintains global thermal equilibrium during the expansion. Thus it should be required that the thermal equilibration time scale be short compared to the expansion time scale. It is worth exploring that limit because the only other microscopic calculations that are presently possible demand the opposite limit.[1,2] Realistically the situation is in between, with the two time scales comparable.

Our model is based on the constrained Hartree-Fock theory with a Hamiltonian

$$h' = h_{HF}[\rho] - \lambda_1 r^2 - \lambda_2 \frac{1}{2}(\vec{p}\cdot\vec{r}+\vec{r}\cdot\vec{p}) \qquad (1)$$

where $\lambda_1$ and $\lambda_2$ are independent Lagrange multipliers. If the temperature is not too high, the Hartree-Fock equations have two sets of solutions depending on the starting conditions of the iteration process.[4] One set of wave functions is obtained by using the usual Woods-Saxon potential as an initial guess, while another set is obtained starting from zero potential. This latter is the vapor phase, while the former has a mixture of vapor and liquid.

To derive the dynamic equations of motion we study the expectation values of the operators for the constraining fields. The equations of motion for these operators are given by

$$i\frac{d\langle r^2\rangle}{dt} = \langle[r^2, h_{HF}]\rangle \qquad (2)$$

$$i\frac{d\langle\vec{p}\cdot\vec{r}\rangle}{dt} = \langle[\vec{p}\cdot\vec{r}, h_{HF}]\rangle \qquad (3)$$

The commutators in Eqs. (2,3) only receive contributions from the constraining fields and we arrive at the following expressions

$$\frac{d\langle r^2\rangle}{dt} = 2\lambda_2\langle r^2\rangle \qquad (4)$$

$$\frac{d\langle\vec{p}\cdot\vec{r}\rangle}{dt} = -2\lambda_1\langle r^2\rangle \qquad (5)$$

For the calculation the initial conditions are imposed by starting the system with a negative $\lambda_1$ coefficient and $\lambda_2$=0. The time evolution of the hot system is determined from Eqs. (4) and (5) using the results of the constrained Hartree-Fock calculations. The

Table I. Time evolution of hot nucleus $^{40}$Ca

$E^* = 197$ MeV

| t (fm/c) | $\lambda_1$ (MeV/fm$^2$) | $\lambda_2$ (MeV/ħ) | $r_m$ (fm) | $\langle\vec{p}\cdot\vec{r}\rangle$ (ħ) | T (MeV) | S | $N_L$ (%) | $N_V$ (%) |
|---|---|---|---|---|---|---|---|---|
| 0 | -0.10 | 0.0 | 3.90 | 0. | 6. | 57 | 92 | 8 |
| 20 | -0.03 | 0.78 | 4.07 | 0.31 | 5.5 | 58 | 89 | 11 |
| 40 | 0.04 | 0.96 | 4.46 | 0.45 | 4.6 | 58 | 86 | 14 |
| 60 | 0.09 | 0.52 | 4.84 | 0.29 | 4.0 | 59 | 82 | 18 |
| 80 | 0.10 | -0.24 | 4.93 | -0.14 | 3.8 | 59 | 81 | 19 |
| 100 | 0.06 | -1.36 | 4.57 | -0.62 | 4.2 | 59 | 84 | 16 |

$E^* = 597$ MeV

| t (fm/c) | $\lambda_1$ (MeV/fm$^2$) | $\lambda_2$ (MeV/ħ) | $r_m$ (fm) | $\langle\vec{p}\cdot\vec{r}\rangle$ (ħ) | T (MeV) | S | $N_L$ (%) | $N_V$ (%) |
|---|---|---|---|---|---|---|---|---|
| 0 | -0.20 | 0.0 | 5.21 | 0. | 12. | 116 | 44 | 56 |
| 20 | -0.11 | 1.44 | 5.65 | 1.10 | 10.4 | 117 | 45 | 55 |
| 40 | 0.01 | 1.7 | 6.80 | 1.85 | 7.3 | 117 | 38 | 62 |
| 60 | 0.076 | 1.2 | 8.12 | 1.75 | 6.1 | 120 | 15 | 85 |
| 80 | 0.11 | 0.37 | 8.90 | 0.7 | 5.9 | 121 | 3 | 97 |

results are shown in Table I for two different values of the initial temperature, $T_I$=6 MeV and 12 MeV. The first point to note is that the entropy remains nearly constant during the expansion, although this was not imposed from the outset. Evidently our assumption, that the thermal equilibration time is small compared to the expansion time, insures that the motion is adiabatic in the thermodynamic sense. Of course it is essential that the model includes the collective kinetic energy of expansion for the adiabatic behavior to occur. As noted in Refs. 3 and 5, the entropy will increase when the system enters the region of phase instability, but this cannot be calculated without a detailed description of the clustering. Note also that the temperature decreases rapidly with time during the expansion process. Thus the physics of isothermal processes is not relevant to nuclear vaporization.

Another question of interest is how much of the system is left in a residual nucleus after the initial expansion has stopped. In macroscopic terms, there is a separation between a low and high density phase, the vapor and liquid. The two cases presented in Table I show quite different behavior in this respect. For the case of $T_I$=6 MeV, the attractive forces eventually stop the expansion, leaving a residual nucleus. This is seen by the decrease in $r_m$ after a time t=80fm/c. In contrast, at $T_I$=12 MeV the system is hot enough to expand indefinitely. These results are in accord with the conclusions of Ref. 5, where the change from bound to unbound expansions was found to occur in the vicinity of $T_I$=8 MeV. Thus we see that there is only about 20% vaporization at $T_I$=6 MeV, but complete vaporization at $T_I$=12 MeV. The vapor fraction is plotted as a function of temperature in Fig. 1. The transition region is rather broad, of the order of 6 MeV as determined by the inverse slope of the curve in Fig. 1.

The theory predicts that there is a limiting temperature in the formation of compound nuclei, as is discussed for example in Ref. 6. This might be observable in the energy spectra of light particles emerging from the collision. Two components to the energy distribution may be found, a high temperature component to be associated with the immediate vaporization and a lower temperature component from compound nucleus evaporation. There is some evidence[7] for a limiting temperature in heavy nuclei as high as 5 MeV; our calculations on a much smaller system would give a lower value. A compound nucleus is only formed at temperatures of 8 MeV and lower, and, as may be seen from Table I, there is considerable cooling in the initial expansion phase while the compound nucleus is forming.

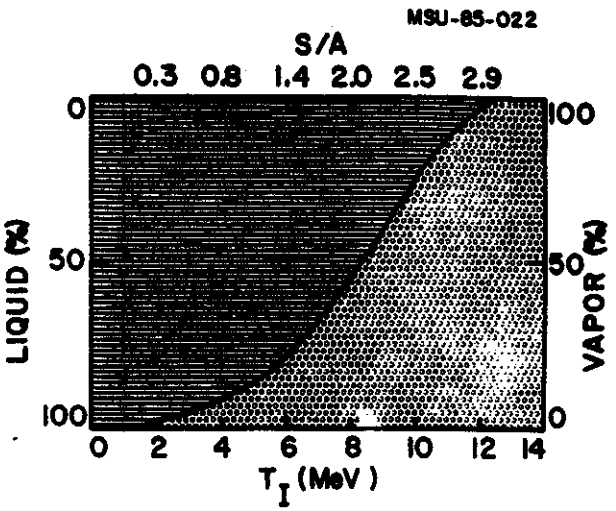


Fig. 1. The ratio of the mass number of the vapor phase to that of the liquid phase. The temperature $T_I$ is that of the beginning of the expansion.

---

* On leave at University of Tennessee and Oak Ridge National Laboratory


1. A. Dhar and S. Das Gupta, Phys. Lett. 137B, 303 (1984).
2. J. Knoll and B. Strack, Phys. Lett. 149B, 45 (1984).
3. A. Vicentini, G. Jacucci, and V. Pandharipande, Univ. of Illinois preprint, 1984.
4. P. Bonche, S. Levit and D. Vautherin, Nucl. Phys. A427, 278 (1984).
5. H. Schultz, et al., Phys. Lett. 147B, 17 (1984).
6. S. Levit and P. Bonche, MIT preprint CTP 1214, (1984).
7. S. Song, et al., Phys. Lett. 130B, 14 (1983).